Applied Catalysis B: Environmental 95 (2010) 320–326

Contents lists available at ScienceDirect

Applied Catalysis B: Environmental

journal homepage: www.elsevier.com/locate/apcatb

Improvement in heat resistance of NOx trap catalyst using Ti–Na binary metal oxide as NOx trap material

Hidehiro Iizuka [a,*], Masato Kaneeda [a], Norihiro Shinotsuka [b], Osamu Kuroda [b], Kazutoshi Higashiyama [a], Akira Miyamoto [c,d]

[a] Hitachi, Ltd. Energy and Environmental Systems Laboratory, 7-2-1 Omika, Hitachi, Ibaraki, 319-1221, Japan
[b] Hitachi, Ltd. Automotive Systems, 2520 Takaba, Hitachinaka, Ibaraki, 312-8503, Japan
[c] Department of Applied Chemistry, Tohoku University, 6-6-11-1302 Aoba, Aramaki, Aoba, Miyagi, 980-8579, Japan
[d] NICHe, Tohoku University, 6-6-11-1302 Aoba, Aramaki, Aoba, Miyagi, 980-8579, Japan

ARTICLE INFO

Article history:
Received 1 October 2009
Received in revised form 7 January 2010
Accepted 13 January 2010
Available online 20 January 2010

Keywords:
NOx trap catalyst
Alkali metals
Alkaline earth metals
Na
Ti
Binary metal oxide
Heat resistance

ABSTRACT

The purpose of this study was to identify suitable base materials for NOx trap catalysts from the viewpoint of heat resistance. First, suitable elements among alkali metals (M: K, Na, Li) and alkaline earth metals (M: Ba, Ca, Sr, Mg) were evaluated using M–Rh,Pt/Al_2O_3. Na was found to be the most suitable element that combines NOx trap performance with hydrocarbon purification performance after heat treatment at 973 K. Moreover, the effects of binary metal oxides with Na and M′ (Zr, Fe, W, Mo, Ti) were evaluated to improve the heat resistance of Na–Rh,Pt/Al_2O_3. The ranking of the NOx trap activity of M′ was Ti > none > Fe > W > Zr > Mo; Ti was the most suitable additional element for improving heat resistance of Na–Rh,Pt/Al_2O_3. The maximum amount of NOx conversion and the maximum number of base sites of Ti,Na–Rh,Pt/Al_2O_3 were reached at a Ti/Na mol ratio of 0.1. It was inferred that the addition of Ti to Na–Rh,Pt/Al_2O_3 formed a Ti–Na binary metal oxide from catalyst characterisation by X-ray diffraction and X-ray photoelectron spectrometry, and this Ti–Na binary metal oxide improved the thermal stability of Na–Rh,Pt/Al_2O_3. Finally, from vehicle tests, it was clear that the NOx trap catalyst, which supported Ti–Na binary metal oxide, exhibited high heat resistance.

1. Introduction

Two results from the reduction of CO_2 emissions, i.e., decrease in fuel consumption, and improvement in exhaust gas purification for automobiles, are desirable for environmental protection. The lean (air-fuel ratio > 18) combustion method used for gasoline engines and the propulsion method used for diesel engines are effective in decreasing fuel consumption. However, nitrogen oxides (NOx) in the exhaust gas cannot be efficiently removed using a conventional three-way catalyst because a large amount of oxygen is present in the exhaust gas.

Therefore, NOx trap catalysts were studied as an alternative and effective NOx purification method [1–4]. NOx trap catalysts generally contain precious metals and base materials on support materials such as alumina [5,6]. This type of catalysts requires lean-rich engine management. In a lean condition, NO is mainly oxidised to NOx on precious metals, and the generated NOx is mainly trapped by the base materials. Next, by switching to a rich condition (air-fuel ratio < 14.7), the trapped NOx is reduced on the precious metals by CO and hydrocarbons (HC) in the exhaust gas. Therefore, there has been considerable interest in these catalysts for lean burn gasoline and diesel engines [7].

Matsumoto et al. [8] studied NOx trap catalysts that supported alkali metals or alkaline earth metals on Pt/Al_2O_3, and concluded that Ba was the most suitable NOx trap material from the viewpoint of simultaneously obtaining good NOx trap ability and HC purification performance. Furthermore, they pointed out that SOx in the exhaust gas converted the NOx trap elements to sulphates, and the sulphates could no longer trap NOx. Since their work, there have been a number of studies on the NOx trap mechanism [9–11] and SOx durability of Pt/Ba/Al_2O_3 [12,13].

When a vehicle is driven with a high load, the temperature of the exhaust gas rises to 973 K. Therefore, the NOx trap catalyst with good NOx purification performance at 673 K and heat resistance at 973 K is necessary. It was reported that NOx trap catalyst with K, whose base strength is stronger than that of Ba, improved the fresh NOx trap ability above 673 K because the NOx trap ability of Ba decreases above 623 K [14]. However, the high temperature causes thermal deterioration of the NOx trap catalyst because of the sintering of precious metals and the reaction of alumina with K and Ba as NOx trap elements [15–17]. There have been some studies on a method to improve the thermal stability of

* Corresponding author. Tel.: +81 294 52 9132; fax: +81 294 52 8803.
E-mail address: hidehiro.iizuka.sq@hitachi.com (H. Iizuka).

0926-3373/$ – see front matter © 2010 Elsevier B.V. All rights reserved.
doi:10.1016/j.apcatb.2010.01.010

K from the viewpoint of inhibiting the reaction of alumina with K [18–20]. Hachisuka et al. [18] pointed out that ZrO_2–TiO_2 support, which maintained a high specific surface area after heat treatment at 1073 K, improved the thermal stability of K and precious metals. Moreover, $MgAl_2O_4$ [19] and Al_2O_3–ZrO_2–TiO_2 [20] were reported to support the thermal stability of K.

The purpose of this study was to improve NOx trap material from the viewpoints of NOx trap performance at 673 K and heat resistance.

First, the most suitable element with respect to heat resistance at 973 K among alkaline metals and alkaline earth metals was evaluated with M–Rh,Pt/Al_2O_3 (M: K, Na, Li, Ba, Ca, Sr, Mg) because the heat treatment temperature was indefinite in a previous study [8].

Next, to improve the heat resistance of M–Rh,Pt/Al_2O_3, the effects of binary metal oxides with M′ (M′ = Zr, Fe, W, Mo, Ti) were investigated. Third, the basicity, the number of base sites, the electronic states, and X-ray crystal structure were examined for characterisation of the binary metal oxide with CO_2 temperature programmed desorption (CO_2 TPD) using an X-ray photoelectron spectrometer (XPS). Finally, the heat resistance catalyst was verified in vehicle tests.

2. Experimental

2.1. Catalyst preparation

The catalytic elements were precious metals (Rh, Pt), alkali metals (K, Na, Li), alkaline earth metals (Ba, Ca, Sr, Mg), and transition metals (Zr, Fe, Ti, W, Mo). These catalytic elements were supported on alumina-coated cordierite honeycombs (Nihongaishi, 400 cells/in^2) using an impregnation method. Pt and Rh were provided by Tanaka Kikinnzoku as $[Pt(NH_3)_2](NO_3)_2$ solution and Rh nitrate solution. Materials provided by Wako Pure Chemicals were $LiNO_3$, $NaNO_3$, KNO_3, $Mg(NO_3)_2{\cdot}6H_2O$, $Ca(NO_3)_2{\cdot}4H_2O$, $Sr(NO_3)_2$, $Fe(NO_3){\cdot}9H_2O$, $(CH_3COO)_2Ba$, $ZrO(NO_3)_2{\cdot}2H_2O$, and $(NH_4)_6\ Mo_7O_{24}{\cdot}4H_2O$. Titania sol was provided by Sakai Chemical Industry, and ammonium metatungstate solution was provided by Nippon Inorganic Colour & Chemical. As an example, Na–Rh,Pt/Al_2O_3 was prepared using the following steps. (1) A wash-coat was deposited by immersing the cordierite honeycomb into an aqueous slurry of boehmite (Sasol, Pural SB). (2) Pt and Rh were supported on the alumina-coated cordierite honeycomb using an impregnation method. The amount of Pt in the alumina-coated honeycomb was 2.8 g/L, and that of Rh was 0.1 g/L. (3) Na was supported on Rh,Pt/Al_2O_3 using the same impregnation method. In each step, the catalyst was dried with a hot air flow, calcined at 873 K for 1 h in an electric furnace, and finally calcined at 973 K for 5 h.

2.2. Catalyst evaluation using model exhaust gas

An ordinary fixed-bed flow reactor was used to examine the catalytic activity of the prepared catalysts. A catalyst (6 cm^3) was placed in a quartz tubular reactor (inner diameter: 28 mm) with a thermocouple placed 10 mm upstream from the catalyst. The catalyst inlet temperature was controlled with an electric furnace, which was vertically fixed to the outside of the tubular reactor. The catalytic performance was measured by exposing the catalyst to synthetic gas mixtures for lean and rich operations, which were controlled with mass flow controllers. Table 1 lists the composition of the lean and rich synthetic gas mixtures. The lean and rich gas flow rate was 3000 cm^3/min (SV: 30,000 h^{-1}).

A steady state experiment was carried out to determine the NOx trap amount of the catalyst under lean operation. The inlet gas temperature was 673 K.

Table 1
Composition of lean and rich simulated experimental gas mixtures.

Gas type	Lean	Rich
NO (ppm)	600	1,000
C_3H_6 (ppm)	500	600
CO (ppm)	1,000	6,000
CO_2 (ppm)	10	12
O_2 (%)	5	0.5
H_2 (ppm)	0	3,300
H_2O (%)	10	10
N_2	Balance	Balance
SV (h^{-1})	30,000	30,000

A lean-rich cycling experiment was carried out to determine NOx and HC conversions. The inlet gas temperature was 673 K, and lean and rich synthetic gas mixtures were alternately introduced for periods of 3 min. The NOx and HC concentrations of the lean or rich atmosphere at the catalyst outlet were measured for 3 min by a chemiluminescence method using an NOx analyser; (Horiba CLA-510) and an FID method using an HC analyser (Horiba FIA-510) after beginning the lean or rich synthetic gas flow. NOx and HC conversions of lean atmosphere were calculated using Eq. (1).

$$\text{NOx (or HC) conversion}\ (\%) = \left(1 - \frac{A}{B}\right) \times 100 \ldots \quad (1)$$

A: total NOx (or HC) concentration of lean atmosphere at the catalyst outlet for 3 min; B: total NOx (or HC) concentration of lean atmosphere at the catalyst inlet for 3 min.

2.3. Catalyst evaluation in vehicle tests

The catalyst was mounted in a commercial lean burn vehicle with a lean burn engine (displacement: 1.8 L). The lean burn vehicle was set on a chassis dynamometer. Catalytic performance was evaluated at steady speeds from 40 to 80 km/h and using a 10–15 mode running based on the Japan Domestic Testing Act. The lean condition areas in the 10–15 mode running were the fixed speed driving areas (20, 40, 60 and 70 km/h) and an acceleration area. Other areas in the 10–15 mode running were maintained in a rich condition. NOx and HC concentrations were measured using an automobile emission analyser (Horiba MEXA-9400).

2.4. Catalyst characterisation

2.4.1. CO_2 TPD

CO_2 is adsorbed on solid surface base sites, and the CO_2 adsorption strength is proportional to the basicity [21]. Therefore, the amount of adsorbed CO_2 corresponds to the number of base sites of the catalyst, and the adsorbed CO_2 sequentially desorbs from weak base sites according to the increase in temperature.

The fixed-bed flow reactor was used for evaluations of both CO_2 adsorption amount and TPD. The powder catalyst (1 mg), from the crushed honeycomb-type catalyst, was placed in the quartz tube reactor (inner diameter: 10 mm) with a thermocouple set 10 mm upstream from the catalyst. The CO_2 concentration was measured using a thermal conductivity detector (TCD) (Hitachi G-103).

The CO_2 adsorption experiment was carried out at 373 K. CO_2 was injected into He carrier every 3 min until CO_2 adsorption was saturated as confirmed by TCD. Then the temperature was increased to 673 K at 10 K/min. During this, only He carrier was used.

2.5. XRD

An X-ray diffractometer (XRD) (Rigaku RU-200) was used to analyse the crystal state of the sample. The Cu Kα radiation X-ray

source was operated at 40 kV and 300 mA and the scan range was 5–90° degrees as 2Θ.

2.6. XPS

An XPS (Shimazu ESCA-5600) was used to analyse the electronic state of the catalysts. The samples were measured under the following conditions: the Al Kα anode X-ray source was operated at 15 kV, analysing diameter was 120 μm, scan speed was 20 eV/min, and scan step was 0.1 eV. The binding energy (BE) of the measured catalyst was corrected at 284.6 eV using the BE from contaminated carbon.

3. Results and discussions

3.1. Catalytic activity of M–Rh,Pt/Al_2O_3

The heat resistance of alkali metal (K, Na, Li) and alkaline earth metal (Ba, Ca, Sr, Mg) as NOx trap elements was evaluated with model gas tests. The concentration of alkali metal on the catalyst was chosen to be twice that of alkaline earth metal because alkali metals are comprised of M_2O-type oxides and alkaline earth metals are comprised of MO-type oxides.

Fig. 1 shows the NOx trap amount of M–Rh,Pt/Al_2O_3 after 973 K heat treatment. The NOx trap amount increased with decreasing electronegativity. Fig. 2 shows HC conversion. The HC conversion markedly decreased when M was K. The addition of base elements to Rh,Pt/Al_2O_3 has been suggested to decrease the propane oxidation performance of precious metals [22]. Therefore, the results for K–Rh,Pt/Al_2O_3 suggested that HC oxidation activity of Rh,Pt/Al_2O_3 markedly decreased due to the basicity of K. The ranking of NOx and HC after 973 K heat treatment was almost equal to those of the catalysts with uncertain heat treatment temperatures [8,23].

It was concluded that Na was the most suitable NOx trap element, which maintained both NOx and HC purification performance after heat treatment at 973 K.

3.2. Catalytic activity of M′,Na–Rh,Pt/Al_2O_3

Improving the heat resistance of Na–Rh,Pt/Al_2O_3 requires improving thermal stability of Na and maintaining the basicity of the NOx trap elements. Thermal stability is improved by raising the melting point of NOx trap element. Melting point and basicity

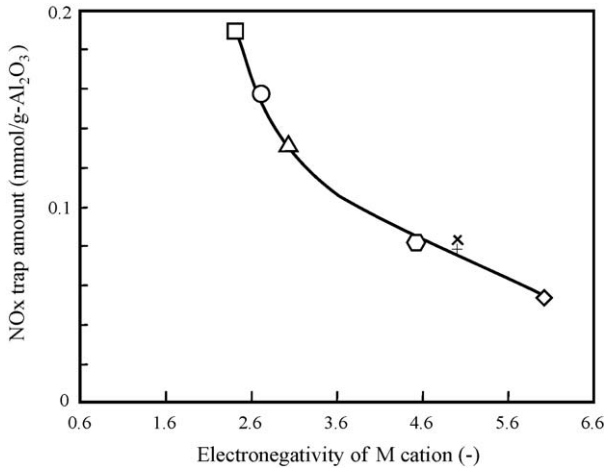

Fig. 1. NOx trap amount of M–Rh,Pt/Al_2O_3; SV—30,000 h^{-1}; M, 0.45 mol/L Li (△); 0.45 mol/L Na (○); 0.45 mol/L K (□); 0.45 mol/L Mg (◇); 0.225 mol/L Ca (×); 0.225 mol/L Sr (+); 0.225 mol/L Ba (⬡); heat treatment conditions, 973 K for 5 h in air.

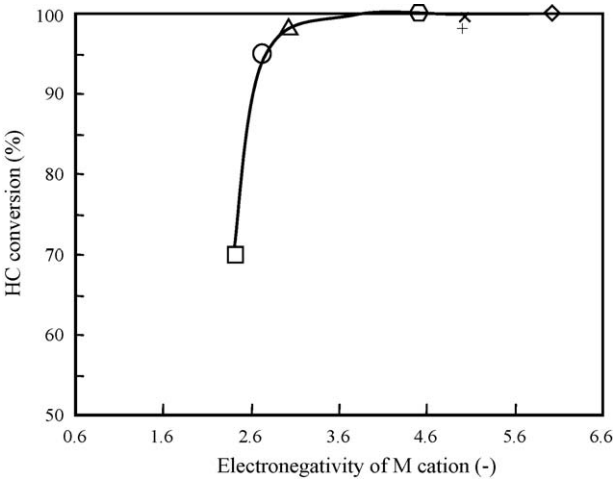

Fig. 2. HC conversion of M–Rh,Pt/Al_2O_3; SV—30,000 h^{-1}; M, 0.45 mol/L Li (△); 0.45 mol/L Na (○); 0.45 mol/L K (□); 0.45 mol/L Mg (◇); 0.225 mol/L Ca (×); 0.225 mol/L Sr (+); 0.225 mol/L Ba (⬡); heat treatment conditions, 973 K for 5 h in air.

are generally in a trade-off relation; for example, Na_2CO_3 basicity is stronger but its melting point is lower (1124 K) than $BaCO_3$, which is less basic but has a higher melting point (1307 K). However, it has been reported that the basicity and thermal stability of binary metal oxides can be controlled by the type and composition of combined elements [24]. Alkali metals make a bronze structure, which is a kind of prevoskite-type binary metal oxide, with Ti, Mo, and W. It has also been reported that the electronic states of the bronze structure differ according to the composition ratio of the binary metal oxide, which affects catalytic activity [25]. Additionally, Fe and Zr also form binary metal oxides with Na. Therefore, Ti, Fe, W, Zr, and Mo were chosen as M′ for M′–Na binary metal oxide that can combine thermal stability with suitable basicity for the NOx trap.

Fig. 3 shows NOx and HC conversions of M′,Na–Rh,Pt/Al_2O_3 for the lean condition after heat treatment at 973 K. The M′/Na molar ratio was 0.1. The amount of Na loading was increased to 0.78 mol/L to improve NOx trap ability. The melting points [26] of M′–Na binary metal oxides are listed in this figure. NOx conversion of Ti,Na–Rh,Pt/Al_2O_3, which forms a binary metal oxide like Na_2TiO_3, whose melting point is higher than that of Na_2CO_3, was superior to NOx conversion of Na–Rh,Pt/Al_2O_3. Moreover, NOx conversions of W,Na–Rh,Pt/Al_2O_3 and Mo,Na–Rh,Pt/Al_2O_3, which form binary metal oxides like Na_2WO_3 and Na_2MoO_3, whose melting points are

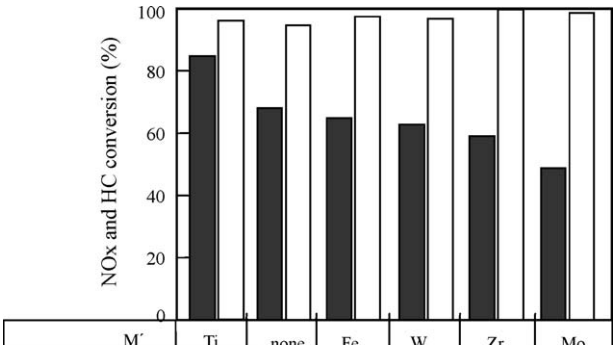

M′	Ti	none	Fe	W	Zr	Mo
Binary metal oxide	Na_2TiO_3	Na_2CO_3	$Na_2Fe_2O_4$	Na_2WO_3	Na_2ZrO_3	Na_2MoO_3
Melting point (K) [20]	1303	1124	-	971	-	960

Fig. 3. NOx and HC conversion of M′,Na–Rh,Pt/Al_2O_3 for lean condition: (■) NOx; (□) HC; SV—30,000 h^{-1}; 0.78 mol/L Na ; M′: Ti, Fe, W, Zr, Mo; M′/Na molar ratio = 0.1; heat treatment conditions, 973 K for 5 h in air.

Table 2
NOx and HC conversion of M′, Na–Rh,Pt/Al_2O_3 for the rich condition at 687 K.

M′	Ti	None	Fe	W	Zr	Mo
NOx conversion (%)	89	89	89	89	86	89
HC conversion (%)	96	94	97	96	99	99

lower than that of Na_2CO_3, were inferior to that of Na–Rh,Pt/Al_2O_3. On the other hand, HC conversion of Ti,Na–Rh,Pt/Al_2O_3 was more than that of Na–Rh,Pt/Al_2O_3.

From these NOx trap results and the melting points of binary metal oxides, the following could be said.

(1) For NOx trap activity of M′,Na–Rh,Pt/Al_2O_3, the order of M′ was: Ti > none > Fe > W > Zr > Mo.
(2) For the melting points of the binary metal oxides, the order was: Na_2TiO_3 > Na_2CO_3 > Na_2WO_3 > Na_2MoO_3.

Table 2 lists the NOx and HC conversions of M′,Na–Rh,Pt/Al_2O_3 for the rich condition at 673 K. The NOx conversions ranged from 86 to 89%, and the HC conversions ranged from 94 to 99%.

These results showed that Ti was the most suitable additional element for improving heat resistance of Na–Rh,Pt/Al_2O_3 at 973 K. It was possible that Ti formed a Ti–Na binary metal oxide with high thermal stability, and this oxide improved the heat resistance without reducing the basicity of the NOx trap catalyst.

3.3. Effects of Ti/Na mol ratio of Ti,Na–Rh,Pt/Al_2O_3

The dependence of the Ti/Na mol ratio for the base strength of Ti,Na–Rh,Pt/Al_2O_3 was examined using CO_2 TPD, and the catalyst was evaluated using model exhaust gas. The Ti/Na mol ratios of the catalysts were 0.0, 0.1, 0.5, and 1.5, and the calcined temperature of the catalysts was 973 K.

Fig. 4 shows the results of CO_2 TPD of Ti,Na–Rh,Pt/Al_2O_3. Its base strength was classified into three types depending on the desorption temperature range: 373–473 K corresponded to weak base sites; 473–573 K corresponded to middle base sites; and 573–673 K corresponded to strong base sites. The total amount of CO_2 desorbed from Ti,Na–Rh,Pt/Al_2O_3 at a Ti/Na mol ratio of 0.1 between 373 and 673 K was larger than that of Na–Rh,Pt/Al_2O_3, whose Ti/Na mol ratio is 0.0. Moreover, the total amount of CO_2 desorption was largest at a Ti/Na mol ratio of 0.1. Therefore, it was concluded that the total number of base sites of Ti,Na–Rh,Pt/Al_2O_3

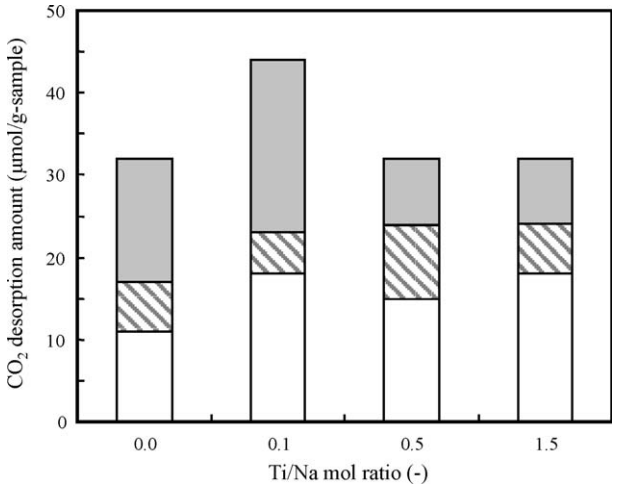

Fig. 4. CO_2 desorption amount of Ti,Na–Rh,Pt/Al_2O_3; CO_2 desorption temperature range, (□) 373–473 K, (▨) 473–573 K, (▩) 573–673 K; 0.78 mol/L Na ; 0.000, 0.078, 0.39,1.17 mol/L Ti; heat treatment conditions, 973 K for 5 h in air.

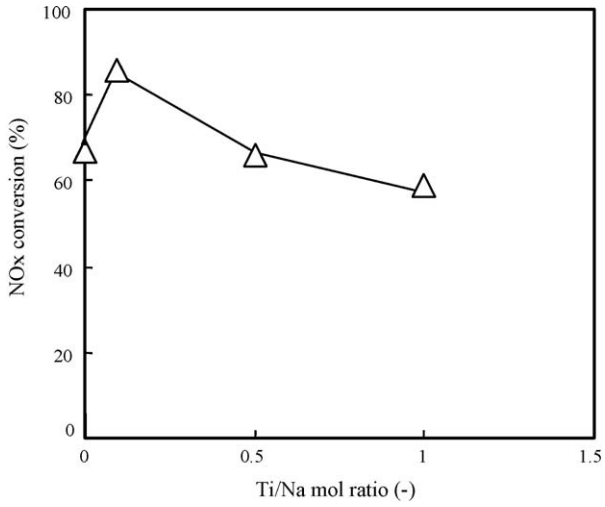

Fig. 5. NOx conversion of Ti,Na–Rh,Pt/Al_2O_3: SV—30,000 h^{-1}; 0.78 mol/L Na ; 0.000, 0.078, 0.39, 0.78 mol/L Ti; heat treatment conditions, 973 K for 5 h in air.

increased more than that of Na–Rh,Pt/Al_2O_3 at the Ti/Na mol ratio of 0.1. Second, the distribution of the base strength of Ti,Na–Rh,Pt/Al_2O_3 was examined. The number of strong base sites increased at a Ti/Na mol ratio of 0.1. However, when the mol ratio was more than 0.1, the number of strong base sites of Ti,Na–Rh,Pt/Al_2O_3 decreased below that of Na–Rh,Pt/Al_2O_3. On the other hand, the sum of the weak and middle base sites increased at a Ti/Na mol ratio of 0.1 but maintained a constant value (about 24 μmol/g-sample) at a ratio of more than 0.1.

Fig. 5 shows the NOx conversion for the lean condition as it depends on the Ti/Na mol ratio. The tendency of NOx conversion increased at a Ti/Na mol ratio of up to 0.1 but decreased at a ratio of more than 0.1. The tendency of NOx conversion at the different Ti/Na mol ratios corresponded with the number of strong base sites. Moreover, NOx conversion for the rich condition was maintained at 89% on either side of the Ti/Na mol ratio of 0.1.

Therefore, it was likely that NOx of the lean atmosphere combustion was trapped on the strong base sites of NOx trap material, and the total number of the base sites of NOx trap material was probably increased by the formation of Ti–Na binary metal oxide at a Ti/Na mol ratio of 0.1, which was an appropriate value. However, when the Ti/Na mol ratio was more than 0.1, the number of strong base sites decreased so that the amount of Ti–Na binary metal oxide in the NOx trap material increased dramatically.

3.4. Characterisation of Ti–Na binary metal oxide

It has been reported that Ti–Na binary metal oxide forms a bronze-type oxide with an amorphous structure [27]. Therefore, the basicity, number of base sites, electronic state, and X-ray crystal structure of Na–Rh,Pt/Al_2O_3 and Ti,Na–Rh,Pt/Al_2O_3 (Ti/Na mol ratio 0.1), which were treated at 973 K for 5 h, were examined using XPS and XRD.

First, the Ti and Na crystal structure on Al_2O_3 was measured using XRD; Ti,Na–Rh,Pt/Al_2O_3 was used to clarify this crystal structure (Fig. 6).

Graham et al. [28] pointed out that $Ba(NO_3)_2$-impregnated alumina formed $BaAl_2O_4$ after heat treatment at 1023 K. Stoica et al. [29] pointed out that when aqueous solutions of $Al(NO_3)_3{\cdot}9H_2O$ and Na_2CO_3 were calcined at 973 K for 2 h, $NaAlO_2$ or $Na_2Al_2O_4$ was formed. However, Pt and Al_2O_3 were identified by XRD analysis of Ti,Na–Rh,Pt/Al_2O_3, as shown in Fig. 6. This result suggested that for Ti,Na–Rh,Pt/Al_2O_3 the reaction with alumina was inhibited due to the presence of Ti.

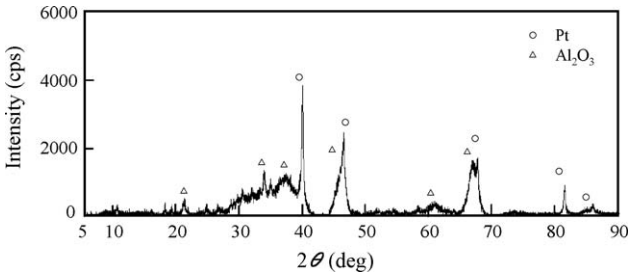

Fig. 6. XRD pattern of Ti,Na–Rh,Pt/Al_2O_3: 0.78 mol/L Na; 0.078 mol/L Ti; heat treatment conditions, 973 K for 5 h in air.

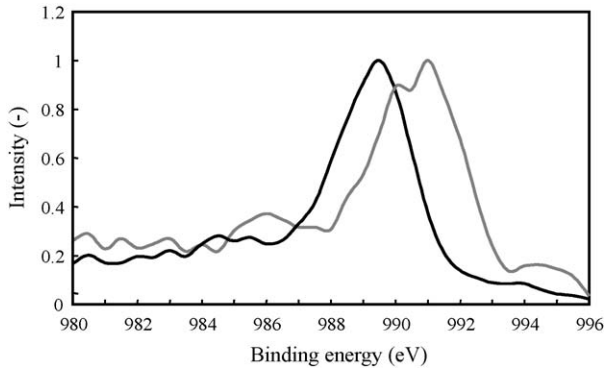

Fig. 7. XPS spectra of Na Auger (KLL): (—) Ti, Na–Rh,Pt/Al_2O_3; (—) Na–Rh,Pt/Al_2O_3; 0.78 mol/L Na; 0.078 mol/L Ti; heat treatment conditions, 973 K for 5 h in air.

On the other hand, alkali metal (M) and M′ (e.g. V, Mn, Mo, W, Ti) form bronze-type binary metal oxides (MxM′yOz), and M oxide is distributed between M′ oxide layers [30]. The M/M′ ratio changes the electronic property of the bronze [31]. It was also reported that Na forms a bronze structure with V [31] and Ti [27]. El-Naggar et al. [27] used XRD analysis and found that Na and Ti form amorphous bronze-type binary metal oxides.

Therefore, it was likely that the Ti–Na binary metal oxide was an amorphous structure similar to bronze-type oxides, or it was thinly supported on the alumina support.

Second, the electronic states of Na–Rh,Pt/Al_2O_3, Ti,Na–Rh,Pt/Al_2O_3, and Na_2TiO_3 (Soekawa Chemicals, purity > 99%) were examined using XPS. Na_2TiO_3 was measured as a reference sample for Ti–Na binary metal oxide. The XPS reference data are quoted from Perkin-Elmer's handbook [32]. Fig. 7 shows the XPS spectra of Na–Rh,Pt/Al_2O_3 and Ti,Na–Rh,Pt/Al_2O_3 in Na Auger (KLL). For Na compounds, those compounds that cannot be identified by Na 1s can be identified in Na Auger (KLL) because the chemical shift of Na Auger (KLL) is larger than that of Na 1s [33]. Therefore, Na Auger (KLL) was used in this study. The peak position of the Na Auger (KLL) BE of Na–Rh,Pt/Al_2O_3 was 989.5 eV, and that of Ti,Na–Rh,Pt/Al_2O_3 was 991.0 eV. Moreover, that of Na_2TiO_3 was 990.2 eV (not shown in Fig. 6). Table 3 summarises the Na Auger (KLL) BE data.

Table 3
Na Auger (KLL) binding energy of Na compounds and NOx trap catalysts.

Compound	Na Auger (KLL) binding energy (eV)	
Na_2O	989.8	Ref. [22]
Na_2CO_3	989.8	
Na_2SeO_3	991.0	
$NaBiO_3$	990.9	
Na	994.3	
Na_2TiO_3	990.2	This work
Na–Rh,Pt/Al_2O_3	989.2	
Ti,Na–Rh,Pt/Al_2O_3	990.5	

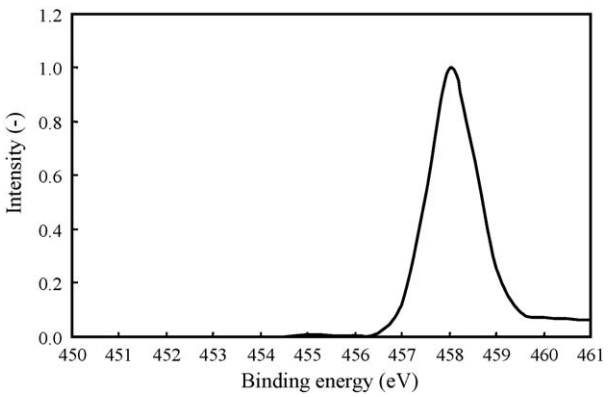

Fig. 8. XPS spectrum of Ti $2p_{3/2}$ of Ti, Na–Rh,Pt/Al_2O_3; 0.78 mol/L Na; 0.078 mol/L Ti; heat treatment conditions, 973 K for 5 h in air.

The Na Auger (KLL) BE of M′–Na binary metal oxides was 990.2–991.0 eV. The Na Auger (KLL) BE of Ti,Na–Rh,Pt/Al_2O_3 was different from that of Na–Rh,Pt/Al_2O_3, and was in the range of that of M′–Na binary metal oxides.

Fig. 8 shows the XPS spectrum of Ti,Na–Rh,Pt/Al_2O_3 in the Ti $2p_{3/2}$ region. The peak position of the Ti $2p_{3/2}$ BE of Ti,Na–Rh,Pt/Al_2O_3 was 458.2 eV. Table 4 summarises the data of Ti $2p_{3/2}$ BE. The Ti $2p_{3/2}$ BE of Ti-M binary metal oxides was 457.8–458.9 eV, and was different from that of TiO_2. The Ti $2p_{3/2}$ BE of Ti,Na–Rh,Pt/Al_2O_3 was in the range of that of Ti–M binary metal oxides.

It was inferred that the Na Auger (KLL) BE and Ti $2p_{3/2}$ BE of Ti,Na–Rh,Pt/Al_2O_3 did not agree with those of Na_2O, Na_2CO_3, TiO_2, and Na_2TiO_3 because Na oxide, which was distributed between Ti oxide layers, electronically interacted with Ti oxide as the Ti–Na binary metal oxide which was not a complete Na_2TiO_3 crystal.

The conclusions on the characterisation of Ti,Na–Rh,Pt/Al_2O_3 and Na–Rh,Pt/Al_2O_3 by XRD and XPS were the following.

(1) It was inferred that the addition of Ti to Na–Rh,Pt/Al_2O_3 formed a Ti–Na binary metal oxide.
(2) Ti–Na binary metal oxide improved the thermal stability of Na and controlled the reduction in the number of the strong base sites after heat treatment at 973 K.

3.5. Vehicle tests

The catalysts, which supported NOx trap materials on Rh,Pt/Al_2O_3, were used to examine the fundamental properties of the NOx trap materials with model gas tests. Finally, practicable heat resistance of the catalyst that supported Ti–Na binary metal oxide, Rh, Pt, and Ce on alumina was verified with vehicle tests. Ce is one of the components of a three-way catalyst, and the role of Ce is to reduce NOx in the rich condition.

The NOx conversion of the catalyst was evaluated at three steady vehicle speeds with other conditions as listed in Table 5. Fig. 9 shows the results for the catalyst that was calcined at 973 K for 5 h in air. The NOx conversion in the lean condition was

Table 4
Ti $2p_{3/2}$ binding energy of Ti compounds and NOx trap catalysts.

Compound	Ti $2p_{3/2}$ binding energy (eV)	
TiO_2	454.1	Ref.[22]
$BaTiO_3$	458.5	
$CaTiO_3$	458.9	
$SrTiO_3$	458.8	
Ti	458.8	
Na_2TiO_3	457.8	This work
Ti,Na–Rh,Pt/Al_2O_3	458.2	

Table 5
Vehicle test conditions at steady speed.

Speed (km/h)	Period of time (s)		Inlet exhaust gas temperature (K)
	Lean	Rich	
40	67	10	623
60	40	7	673
80	30	5	823

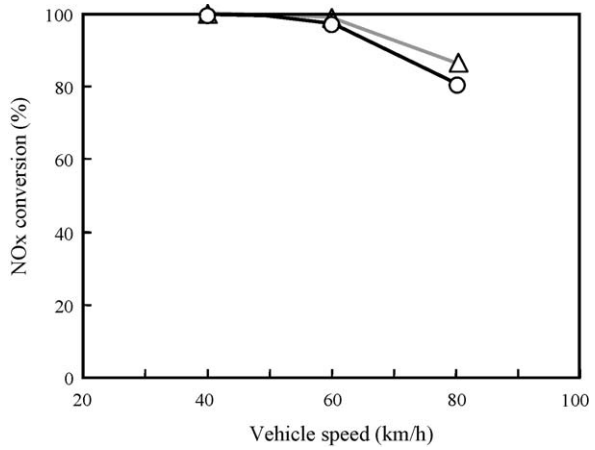

Fig. 9. NOx conversions of Ti,Na–Rh,Pt–Ce/Al_2O_3 at constant vehicle speed from 40 to 80 km/h: (○) total NOx conversion in lean and rich conditions: (△) NOx conversion in lean condition; 0.78 mol/L Na ; 0.078 mol/L Ti; 0.19 mol/L Ce, 0.1 g/L Rh; 2.8 g/L Pt; heat treatment condition, 973 K for 5 h in air.

maintained at more than 99% from 40 km/h (627 K) to 60 km/h (673 K) and at 85% at 80 km/h (723 K). The total NOx conversion in lean and rich conditions was maintained at more than 97% at 40 km/h (627 K) and 60 km/h (673 K), in contrast, it was 80% at 80 km/h (723 K). Because the vehicle speed for the 10–15 mode running is 0–70 km/h, the catalyst will maintain high total NOx purification performance. Therefore, the NOx and HC purification performance of the Ti–Na binary metal oxide-supported catalyst was evaluated according to the 10–15 mode running. The heat treatment conditions were 873, 973, 1073, and 1173 K for 5 h in air. NOx and HC conversions were both maintained at more than 90% up to 1073 K (Fig. 10).

Therefore, the test results showed that the catalyst, which supported Ti–Na binary metal oxide as the NOx trap material, combined high NOx purification performance with high heat resistance in the vehicle tests.

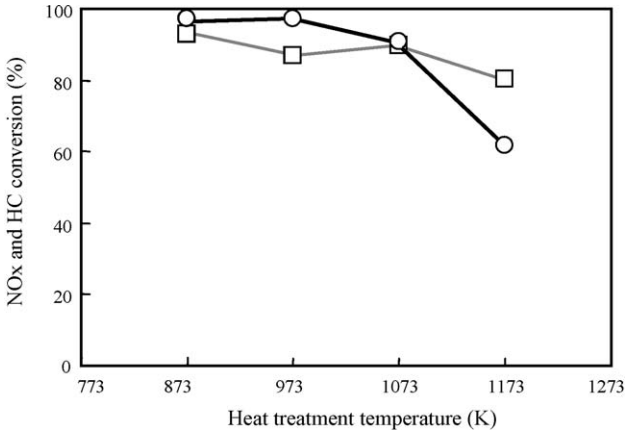

Fig. 10. NOx and HC conversions of Ti,Na–Rh,Pt–Ce/Al_2O_3 with vehicle test: (○) NOx; (□) HC; 0.78 mol/L Na ; 0.078 mol/L Ti; 0.19 mol/L Ce, 0.1 g/L Rh; 2.8 g/L Pt; heat treatment conditions, 873, 973,1073 and 1173 K for 5 h in air.

4. Conclusions

The NOx trap material to improve heat resistance of NOx trap catalysts was examined using model gas tests, CO_2 TPD, XRD, XPS, and vehicle tests.

(1) Among M–Rh,Pt/Al_2O_3 compounds where M was an alkali metal (K, Na, Li) or an alkaline earth metal (Ba, Ca, Sr, Mg), Na–Rh,Pt/Al_2O_3 had NOx trap performance comparable with HC purification performance after heat treatment at 973 K.
(2) To improve the heat resistance of Na–Rh,Pt/Al_2O_3, the effects of binary metal oxides with Na and M′ (M′: Zr, Fe, W, Mo, Ti) were examined. The ranking of the NOx trap activity of M′ was Ti > none > Fe > W > Zr > Mo; Ti was the most suitable additional element for improving heat resistance of Na–Rh,Pt/Al_2O_3.
(3) The maximum amount of NOx conversion and the maximum number of base sites of Ti,Na–Rh,Pt/Al_2O_3 were reached at a Ti/Na mol ratio of 0.1.
(4) It was inferred that the addition of Ti to Na–Rh,Pt/Al_2O_3 formed a Ti–Na binary metal oxide from catalyst characterisation by XRD and XPS, and Ti–Na binary metal oxide improved the thermal stability of Na–Rh,Pt/Al_2O_3.
(5) The NOx trap catalyst that supported Ti–Na binary metal oxide combined high NOx purification performance with high heat resistance in vehicle tests.

Appendix A. Supplementary data

Supplementary data associated with this article can be found, in the online version, at doi:10.1016/j.apcatb.2010.01.010.

References

[1] D.R. Monroe, C.L. Dimaggio, D.D. Beck, F.A. Matekunas, SAE (1993) 930737.
[2] N. Miyoshi, S. Matsumoto, Studies in Surface Science and Catalysis 121 (1999) 245.
[3] W. Bögner, M. Krämer, B. Krutzsch, S. Pischinger, D. Voigtländer, G. Wenninger, F. Wirbeleit, M.S. Brogan, R.J. Brisley, D.E. Webster, Applied Catalysis B: Environmental 7 (1995) 153.
[4] H. Iizuka, M. Kaneeda, K. Higashiyama, O. Kuroda, N. Shinotsuka, H. Watanabe, H. Ohno, T. Takanohashi, N. Satoh, SAE (2004), 2004-01-1495.
[5] L. Lietti, P. Forzatti, I. Nova, E. Tronconi, Journal of Catalysis 204 (2001) 175.
[6] N. Iwata, Y. Suzuki, H. Kato, M. Takeuchi, A. Sugiura, SAE (2004), 2004-01-1494.
[7] J. McDonald, B. Bunker, SAE (2002), 2002-01-2877.
[8] S. Matsumoto, H. Watanabe, T. Tanaka, A. Isogai, K. Kasahara, Journal of Chemical Society of Japan 12 (1996) 997.
[9] P. Broqvist, H. Gronbeck, E. Fridell, I. Panas, Catalysis Today 96 (2004) 71.
[10] K.S. Kabin, R.L. Munfrief, M.P. Harold, Catalysis Today 96 (2004) 79.
[11] C.M.L. Scholz, V.R. Gangwal, J.H.B.J. Hoebink, J.C. Schouten, Applied Catalysis B: Environmental 70 (2007) 226.
[12] C. Sedlmair, K. Seshan, A. Jentys, J.A. Lercher, Catalysis Today 75 (2002) 413.
[13] A. Amberntesson, M. Skoglundh, S. Ljungström, E. Friell, Journal of Catalysis 217 (2003) 253.
[14] Y.-W. Kim, J. Sun, H. Koimanovsky, J. Koncsol, SAE (2003), 2003-01-1164.
[15] A. Amberntesson, E. Friell, M. Skoglundh, Applied Catalysis B: Environmental 46 (2003) 429.
[16] J.R. Theis, J.A. Ura, G.W. Graham, H.–W. Jen, J.J. Li, W.L. Waktins, C.T. Goralski Jr., SAE (2004), 2004-01-1493.
[17] K. Yamazaki, N. Takahashi, H. Shinjoh, M. Sugiura, Applied Catalysis B: Environmental 53 (2004) 1.
[18] I. Hachisuka, T. Yoshida, H. Ueno, N. Takahashi, A. Suda, M. Sugiura, SAE (2002), 2002-01-0732.
[19] N. Takahashi, S. Matsunaga, T. Tanaka, H. Sobukawa, H. Shinjoh, Applied Catalysis B: Environmental 77 (2007) 73.
[20] H. Imagawa, N. Takahashi, T. Tanaka, S. Matsunaga, H. Shinjoh, Applied Catalysis B: Environmental 92 (2009) 23.
[21] K. Tanaka, A. Ozaki, Catalysts & Catalysis 6 (1964) 262.
[22] Y. Yazawa, H. Yoshida, S. Komai, T. Hattori, Applied Catalysis A: General 233 (2002) 103.
[23] S. Matsumoto, New Ceramics 11 (1998) 13.

[24] K. Tanabe, M. Misono, Y. Ono, H. Hattori, New Solid Acids and Bases: Their Catalytic Properties, Elsevier Science Publishers, 1989,, p. 112.
[25] Y. Saito, T. Mizoroki, I. Yasumori, M. Yamaguchi, Y. Yoneda, Kikan Kagaku Sosetsu 34 (1998) 6418.
[26] Y. Iwasawa, Kagaku Binran Kiso I (Handbook of Chemistry, Basic Ed. I), Maruzen, 1993,, p. I-18.
[27] I.M. El-Naggar, E.A. Mowafy, I.M. Ali, H.F. Aly, Adsorption 8 (2002) 2251.
[28] G.W. Graham, H.–W. Jen, W. Chun, H.P. Sun, X.Q. Pan, R.W. McCabe, Catalysis Letters 93 (2004) 129.
[29] G. Stoica, S. Abello, J. Perz-Ramirez, Applied Catalysis A: General 365 (2009) 252.
[30] S. Nagakura, Y. Iguchi, Y. Ezawa, S. Iwamura, R. Kubo, Physics and Chemistry Encyclopedia Ver.5, Iwanami, 2001,, p. 1220.
[31] M. Isobe, Y. Ueda, Y. Oka, T. Yao, Journal of Solid State Chemistry 145 (1999) 361.
[32] J.F. Moulder, W.F. Sticle, P.E. Sobol, K.D. Bomben, Handbook of X-ray Photoelectron Spectroscopy, Perkin-Elmer Corporation Physical Electronics Division, 1992, p. 288.
[33] H. Mojushiro, Journal of the Association of Materials Engineering for Resources 18 (2003) 1.